Crystal Dynamics of Copper*

E. C. SVENSSON,† B. N. BROCKHOUSE, AND J. M. ROWE‡
Department of Physics, McMaster University, Hamilton, Ontario, Canada
(Received 12 August 1966)

The frequency/wave-vector dispersion relation for the symmetry directions [00ζ], [0ζζ], [ζζζ], and [0ζ1] in copper at room temperature has been determined by inelastic neutron scattering. Interplanar and atomic force constants have been obtained. First-neighbor interactions are dominant, but longer range forces, extending to at least sixth-nearest neighbors, are also present. Physically realistic errors have been assigned to many of the force constants; to our knowledge this has not been done previously. The analysis of the data, and the excellent agreement between measurements carried out at the Chalk River and McMaster University reactors, indicate that, on the average, the errors conventionally assigned to frequencies in neutron-scattering studies are too large by about a factor of 2 to be standard deviations. Frequency distributions have been obtained and used to calculate various thermodynamic quantities which agree quite well with experiment. (Discrepancies of a few percent appear to be accounted for by anharmonic effects.) Our results are in rather good agreement with those of Sinha obtained by quite different experimental methods.

I. INTRODUCTION

IN connection with a recent study of the crystal dynamics of dilute alloys of gold in copper,[1] accurate values of certain normal-mode frequencies for copper were required. The frequency distribution for copper was also needed in order to compare the alloy results with the predictions of the theory of Elliott and Maradudin.[2] The measurements on copper were therefore extended to yield the dispersion relation for the lattice vibrations with wave vectors along the four major symmetry directions [00ζ], [0ζζ], [ζζζ], and [0ζ1]. All measurements were carried out at room temperature (296°K). The results have additional interest in that copper is probably the simplest of the face-centered cubic metals, and, as such, is a logical choice for theoretical studies.[3] Force-constant models have been constructed from the results by a procedure which gives the best mathematical fit to the data, and which also allows one to assign physically realistic errors to the largest possible number of force constants. First-neighbor interactions are dominant, but there is also a weak longer range force system with interactions extending to at least sixth-nearest neighbors. Frequency distributions obtained from the force-constant models were used to calculate various thermodynamic quantities which agree quite well with experiment. (The small discrepancies appear to be accounted for by anharmonic effects.)

Several neutron scattering studies of the lattice vibrations in copper have been carried out by other workers,[4–8] and Jacobsen[9] has studied the dispersion relation by the diffuse scattering of x rays. However, except for the work of Sinha and Squires,[4] the results of these studies have been incomplete and somewhat inaccurate. Sinha and Squires[4] have carried out extensive measurements (476 frequencies), largely at off-symmetry positions in reciprocal space. Although their results for the symmetry directions are unevenly distributed as to wave vector, branch, and direction, and their quoted errors are two to five times larger than ours, there is generally good agreement where overlap with our results occurs. Even more important is the good agreement between their force constants, determined mainly by off-symmetry results, and our force constants, determined completely by results for the symmetry directions.

Work on copper at room temperature and at lower temperatures is also in progress at Oak Ridge National Laboratory.[10]

The frequencies ν and wave vectors $\mathbf{q}$ of the normal modes of vibration of a crystal are connected by the

* Work supported by a grant from the National Research Council of Canada.

† Holder of a National Research Council of Canada Studentship. Present address: Neutron Physics Branch, Atomic Energy of Canada Limited, Chalk River, Ontario, Canada.

‡ Holder of a National Research Council of Canada Studentship. Present address: Solid State Science Division, Argonne National Laboratory, Argonne, Illinois.

[1] E. C. Svensson, B. N. Brockhouse, and J. M. Rowe, Solid State Commun. **3**, 245 (1965).

[2] R. J. Elliott and A. A. Maradudin, in *Inelastic Scattering of Neutrons in Solids and Liquids* (International Atomic Energy Agency, Vienna, 1965), Vol. 1, p. 231.

[3] See, e.g., T. Toya, in *Inelastic Scattering of Neutrons in Solids and Liquids* (International Atomic Energy Agency, Vienna, 1965), p. 25; H. C. White, Phys. Rev. **112**, 1092 (1958); and the references contained in these two articles.

[4] S. K. Sinha, Phys. Rev. **143**, 422 (1966); see also S. K. Sinha and G. L. Squires, *Lattice Dynamics*, edited by R. F. Wallis (Pergamon Press, Ltd., London, 1965), p. 53.

[5] D. Cribier, B. Jacrot, and D. Saint-James, in *Inelastic Scattering of Neutrons in Solids and Liquids* (International Atomic Energy Agency, Vienna, 1961), p. 549.

[6] E. Maliszewski, J. Sosnowski, K. Blinowski, J. Kozubowski, I. Padlo, and D. Śledziewska, in *Inelastic Scattering of Neutrons in Solids and Liquids* (International Atomic Energy Agency, Vienna, 1963), Vol. 2, p. 87.

[7] E. Z. Vintaikin, V. V. Gorbachev, and P. L. Gruzin, Fiz. Tverd. Tela **7**, 367 (1965) [English transl.: Soviet Phys.—Solid State **7**, 296 (1965)].

[8] T. Schneider and E. Stoll, Solid State Commun. **4**, 79 (1966).

[9] E. H. Jacobsen, Phys. Rev. **97**, 654 (1955).

[10] R. M. Nicklow and L. J. Raubenheimer (private communications); see also R. M. Nicklow, G. Gilat, H. G. Smith, L. J. Raubenheimer, and M. K. Wilkinson, Bull. Am. Phys. Soc. **11**, 263 (1966).

dispersion relation

$$\nu=\nu_j(\mathbf{q}), \tag{1}$$

where j is a branch index. (Throughout this paper we will consider only Bravais crystals so that $j=1,2,3$.) The dispersion relation can be discovered by processes in which slow neutrons interact with the crystal and either create or annihilate one quantum of lattice vibration (phonon). These "one-phonon" processes are governed by the equations of conservation of energy and wave vector (momentum/$\hbar$) between neutron and phonon,

$$E_0-E'=\pm h\nu=\pm\hbar\omega, \tag{2a}$$

$$\mathbf{k}_0-\mathbf{k}'=\mathbf{Q}=2\pi\boldsymbol{\tau}+\mathbf{q}, \tag{2b}$$

where (E_0,E') and $(\mathbf{k}_0,\mathbf{k}')$ are the incoming and outgoing neutron energies and wave vectors, respectively, and $\boldsymbol{\tau}$ is a reciprocal lattice vector. Hence, from the groups in the distribution of neutrons inelastically scattered by the crystal in "one-phonon" processes, one can infer the existence of normal modes of vibration of the crystal with frequencies and wave vectors given by Eqs. (2).

The dispersion relation thus determined may be analyzed in terms of atomic force constants by means of the Born–von Kármán theory of lattice dynamics.[11] According to this theory the angular frequencies ω and the polarization vectors ξ of the normal modes of vibration of the crystal satisfy the equation

$$M\omega^2\xi_\alpha=\sum_\beta \xi_\beta D_{\alpha\beta}(\mathbf{q}), \tag{3}$$

where $\alpha,\beta=1,2,3$ refer to Cartesian components, M is the atomic mass, and the $D_{\alpha\beta}(\mathbf{q})$, the elements of the dynamical matrix, are given by

$$D_{\alpha\beta}(\mathbf{q})=\sum_{L\neq 0}\{-\Phi_{\alpha\beta}(\mathbf{R}_L)\}(1-\cos\mathbf{q}\cdot\mathbf{R}_L), \tag{4}$$

where the $\mathbf{R}_L$ are the vector coordinates of the atoms at their equilibrium positions with respect to the atom at the origin ($L=0$), and the $-\Phi_{\alpha\beta}(\mathbf{R}_L)$ are the atomic force constants. Physically, $-\Phi_{\alpha\beta}(\mathbf{R}_L)$ is the force on the atom at the origin in the direction α when the atom at position $\mathbf{R}_L$ is given a unit displacement in the direction β. From the dispersion relation the forces between atoms in the crystal can therefore be calculated by Eqs. (3) and (4). For a particular branch in a particular symmetry direction, Eqs. (3) and (4) reduce to the form

$$M\omega^2=\sum_n \Phi_n[1-\cos(n\pi q/q_M)], \tag{5}$$

where q_M is defined to be one-half the distance from the origin to the nearest reciprocal lattice point in the direction of $\mathbf{q}$, $q=|\mathbf{q}|$, and the Φ_n are linear combinations of the $-\Phi_{\alpha\beta}(\mathbf{R}_L)$ for which $\mathbf{q}\cdot\mathbf{R}_L$ is constant. Since ($\mathbf{q}\cdot\mathbf{R}_L=$const) defines a plane, the Φ_n are conventionally called interplanar force constants.[12]

The condition for a nontrivial solution of Eq. (3) is

$$\det|D_{\alpha\beta}(\mathbf{q})-M\omega^2\delta_{\alpha\beta}|=0, \tag{6}$$

where $\delta_{\alpha\beta}=1$ if $\alpha=\beta$, and is zero otherwise. If the atomic force constants are known, then so are the $D_{\alpha\beta}(\mathbf{q})$ from Eq. (4), and, solving Eq. (6) for a great many values of $\mathbf{q}$ in the irreducible 1/48 of the first Brillouin zone, a histogram representation of the frequency distribution $g(\nu)$ can be obtained. Various approximate methods, which greatly decrease the computational time required to calculate a given number of frequencies, are available.[13,14]

Having obtained $g(\nu)$, one may readily calculate the moments of the frequency distribution

$$M_n=\int \nu^n g(\nu)d\nu, \quad \text{for} \quad n>-3, \tag{7}$$

and the Debye frequencies

$$\nu_n=[(n+3)M_n/3]^{1/n}, \quad \text{for} \quad n\neq 0,-3, \tag{8a}$$

$$\nu_0=\exp\left[\frac{1}{3}+\int g(\nu)\ln\nu d\nu\right], \tag{8b}$$

and

$$\nu_{-3}=(k_B/h)\Theta_D(0^\circ\mathrm{K})=(3/b)^{1/3}, \tag{8c}$$

where b is determined by the low-frequency expansion of $g(\nu)$,

$$g(\nu)=b\nu^2+\cdots. \tag{9}$$

One may also calculate the lattice specific heat at constant volume,

$$\frac{C_v(T)}{3Nk_B}=\int\frac{(\beta h\nu)^2 g(\nu)\exp(\beta h\nu)d\nu}{[\exp(\beta h\nu)-1]^2}, \tag{10}$$

(where $\beta=1/k_BT$ and k_B is Boltzmann's constant) and the Debye-Waller coefficient,

$$2W(T)=\nu_R\int\nu^{-1}\coth(\tfrac{1}{2}\beta h\nu)g(\nu)d\nu, \tag{11}$$

where $h\nu_R=\hbar^2Q^2/2M$ is the recoil energy of a free atom of mass M. Using $C_v(T)$ calculated from Eq. (10) and the Debye-theory formula,

$$\frac{C_v(T)}{3Nk_B}=3\left(\frac{T}{\Theta_D}\right)^3\int_0^{\Theta_D/T}\frac{x^4e^x dx}{(e^x-1)^2}, \tag{12}$$

[11] See, e.g., M. Born and K. Huang, *Dynamical Theory of Crystal Lattices* (Clarendon Press, Oxford, England, 1954).

[12] A. J. E. Foreman and W. M. Lomer, Proc. Phys. Soc. (London) **B70**, 1143 (1957).

[13] G. Gilat and G. Dolling, Phys. Letters 8, 304 (1964).

[14] G. Gilat and L. J. Raubenheimer, Phys. Rev. 144, 390 (1966).

one obtains the Debye temperature $\Theta_D(T)$ by iteration.

In Eqs. (7)–(11) it is assumed that $g(\nu)$ is normalized so that $\int g(\nu)d\nu=1$, and the integration is over the range $0\leqslant\nu\leqslant\nu_M$ where ν_M is the maximum frequency in the spectrum. In performing the calculations, one of course replaces the integration by a summation and expands the integral of Eq. (12) in the series that converges most rapidly for the range of interest of Θ_D/T.

II. MEASUREMENTS AND RESULTS

The majority of the measurements were carried out using the triple-axis crystal spectrometer at the N.R.U. reactor at Chalk River in the "constant-**Q**" mode[15] of operation with fixed E'. In order to avoid spurious neutron groups arising from second-order reflections from the analyzing crystal (i.e., reflections for which $E_0\pm h\nu=4E'$), and to also maintain good resolution, almost all of the work was done with the analyzing crystal set at $2\theta_A=47°$. [θ_A is the Bragg scattering angle and the (111) planes of an aluminum analyzer were used.] The (200) planes of an aluminum monochromator were used throughout, and all measurements were made at neutron energy loss (phonon creation). Two specimen crystals were employed, and each was studied in two orientations—with either a (100) or a (1$\bar{1}$0) plane of the reciprocal lattice in the plane of the spectrometers. The crystals were supplied by Research Crystals Incorporated, Richmond, Virginia. The crystal used for most of the measurements was a cylinder, 1 in. in diameter $\times 2\frac{3}{8}$ in. long, with a (100) crystallographic axis about 1° off the cylinder axis. The other crystal was an approximate sphere of 1-in. diameter which had been machined from another cylindrical crystal. Extensive measurements of the [00ζ]T branch carried out using the second crystal have been published previously.[1]

The low-wave-vector regions of the [0$\zeta\zeta$]T_1 and L branches have been studied on the new triple-axis spectrometer at the McMaster University reactor. The T_1 branch was studied at high resolution—fixed E_0, with $2\theta_M=61.86°$, and variable E', with $62°\leqslant 2\theta_A\leqslant 110°$. [$\theta_A$ and θ_M are the Bragg scattering angles for the analyzer and monochromator respectively, and (200) planes of copper crystals were used for both.] The L branch was studied using the same analyzer and monochromator, but at a lower resolution—$2\theta_M=48.9°$. Both "constant-**Q**" and "constant-E" modes of operation[15] were employed.

In Figs. 1 and 2 the (100) and (1$\bar{1}$0) planes of the reciprocal lattice of copper are shown together with typical neutron groups measured at Chalk River. The lines through the points are drawn by hand and do not represent any fitting procedure. Two groups are shown for each of the [0$\zeta\zeta$]T_1 and T_2 and the [00ζ]T branches

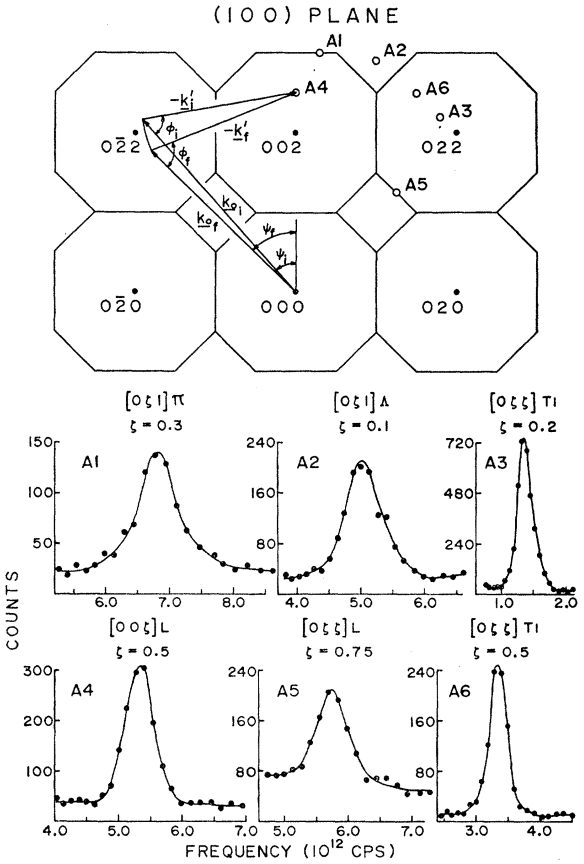

FIG. 1. The (100) plane of the reciprocal lattice and several typical neutron groups for copper obtained in "constant-**Q**" experiments such as the one shown for group A4. The groups are labeled with the branch designation and the value of the reduced wave vector ζ. Note that the vectors labeled $-k'_f$, etc. are actually $-ak'_f/2\pi$, etc. where a is the lattice constant (this also applies to Fig. 2).

as an illustration of how the width changes with frequency and slope along the same branch. The change with frequency is much slower than the change with slope and arises primarily from the change in energy resolution as $2\theta_M$ is varied ($\Delta E_0/E_0=2\Delta\theta_M\cot\theta_M$, where $\Delta\theta_M$ is determined mainly by the collimators used and is essentially constant). The width changes rapidly with slope because the focusing[16] is critically dependent on the slope. The focusing for transverse branches is more complete than for longitudinal branches, as is quite apparent from the groups shown. In each of Figs. 1 and 2 the initial and final vector diagrams are shown for a "constant-**Q**" experiment designed to measure one of the neutron groups shown at the bottom of the figure (i.e., group A4 for Fig. 1 and group B5 for Fig. 2).

In several cases the same normal mode was studied in both planes of the reciprocal lattice and/or in both crystals and/or at both Chalk River and McMaster

[15] B. N. Brockhouse, in *Inelastic Scattering of Neutrons in Solids and Liquids* (International Atomic Energy Agency, Vienna, 1961), p. 113.

[16] M. F. Collins, Brit. J. Appl. Phys. **14**, 805 (1963).

TABLE I. Normal-mode frequencies (in units of 10^{12} cps) for the symmetry branches[a] in copper at 296°K.

$[00\zeta]T$		$[00\zeta]L$		$[0\zeta\zeta]T_2$	
ζ	ν	ζ	ν	ζ	ν
0.15	1.17±0.04	0.15	1.90±0.09	0.1	1.11±0.03
0.2	1.56±0.04	0.2	2.42±0.07	0.15	1.69±0.04
0.25	1.92±0.04	0.25	3.02±0.08	0.2	2.27±0.04
0.275	2.12±0.04	0.3	3.56±0.06	0.25	2.82±0.04
0.3	2.30±0.04	0.4	4.47±0.07	0.3	3.37±0.04
0.35	2.64±0.04	0.5	5.32±0.07	0.4	4.30±0.05
0.4	3.01±0.04	0.6	6.05±0.08	0.5	5.07±0.06
0.45	3.30±0.05	0.65	6.37±0.08	0.6	5.71±0.06
0.5	3.62±0.04	0.7	6.60±0.08	0.65	6.04±0.06
0.55	3.88±0.05	0.75	6.77±0.12	0.7	6.31±0.07
0.6	4.15±0.05	0.8	6.99±0.13	0.75	6.54±0.10
0.65	4.34±0.05	0.85	7.14±0.14	0.8	6.80±0.11
0.7	4.54±0.05	0.9	7.17±0.12	0.9	7.13±0.15
0.75	4.73±0.06	1.0	7.19±0.12	1.0	7.19±0.12
0.8	4.86±0.07				
0.9	5.02±0.07				
1.0	5.08±0.08				
$[0\zeta\zeta]T_1$		$[0\zeta\zeta]L$		$[\zeta\zeta\zeta]L$	
ζ	ν	ζ	ν	ζ	ν
0.2	1.35±0.04	0.1	2.03±0.10	0.05	1.24±0.06
0.3	2.03±0.04	0.2	3.70±0.08	0.075	1.86±0.07
0.4	2.70±0.04	0.3	5.11±0.07	0.1	2.46±0.07
0.5	3.34±0.04	0.4	5.97±0.08	0.125	2.99±0.06
0.6	3.89±0.05	0.5	6.36±0.10	0.15	3.59±0.06
0.7	4.34±0.05	0.6	6.38±0.12	0.2	4.54±0.06
0.75	4.55±0.05	0.7	5.91±0.10	0.25	5.43±0.07
0.8	4.75±0.07	0.75	5.73±0.08	0.3	6.14±0.07
0.9	5.03±0.08	0.8	5.51±0.07	0.35	6.67±0.08
1.0	5.08±0.08	0.9	5.19±0.07	0.4	7.06±0.10
		1.0	5.08±0.08	0.45	7.25±0.13
				0.5	7.40±0.13
$[\zeta\zeta\zeta]T$		$[0\zeta 1]\Pi$		$[0\zeta 1]\Lambda$	
ζ	ν	ζ	ν	ζ	ν
0.075	0.79±0.04	0.0	7.19±0.12	0.0	5.08±0.08
0.1	1.01±0.05	0.1	7.17±0.15	0.1	5.03±0.08
0.125	1.23±0.06	0.2	7.07±0.14	0.2	4.99±0.07
0.15	1.47±0.06	0.3	6.80±0.09	0.3	4.97±0.08
0.2	1.87±0.06	0.4	6.44±0.09	0.4	4.89±0.09
0.25	2.29±0.05	0.5	6.10±0.08	0.5	4.89±0.08
0.3	2.66±0.06	0.6	5.77±0.08		
0.35	2.97±0.06	0.7	5.47±0.08		
0.4	3.17±0.07	0.8	5.27±0.08		
0.45	3.34±0.07	0.9	5.13±0.08		
0.5	3.37±0.07	1.0	5.08±0.08		

[a] The polarization vectors for the $[0\zeta\zeta]T_1$ and T_2 branches are parallel to $[0\bar{\zeta}\zeta]$ and $[\zeta 00]$, respectively.

and/or at different equivalent points in the same plane (including both focused and defocused positions). In all cases agreement to well within the assigned errors was obtained. This serves as a check on the alignment and calibration procedures and on other instrumental effects.

The normal-mode frequencies ν and reduced wave vectors ζ for the symmetry direction are given in Tables I and II. The results of Table I were obtained at Chalk River, and the results for the low-wave-vector region of the $[0\zeta\zeta]T_1$ branch given in Table II were obtained at McMaster. The latter study was undertaken partly to check the performance of the new McMaster triple-axis spectrometer and partly to study in detail the $[0\zeta\zeta]T_1$ branch in which an anomaly had been found in similar measurements on palladium.[17] Where equivalent results are given in Tables I and II, it is seen that they agree to well within the combined errors. The errors were assigned to the frequency values by considering the widths and shapes of the corresponding neutron groups, the counting statistics, and possible systematic errors. There is no simple recipe for making these assignments; our (later) analysis indicates that the errors given in Tables I and II, which were arrived at following the philosophy used in several earlier studies,[18–20] are almost certainly overestimates (in the sense of standard deviations), perhaps by as much as a factor of 2.

TABLE II. Normal-mode frequencies (in units of 10^{12} cps) for the low-wave-vector part of the $[0\zeta\zeta]T_1$ branch in copper at 296°K.

ζ	ν	ζ	ν	ζ	ν
0.075	0.51±0.03	0.225	1.48±0.03	0.375	2.50±0.03
0.100	0.67±0.03	0.250	1.64±0.03	0.400	2.67±0.04
0.125	0.81±0.03	0.275	1.82±0.03	0.415	2.77±0.04
0.150	0.99±0.03	0.300	2.00±0.03	0.425	2.89±0.03
0.175	1.16±0.03	0.325	2.18±0.03	0.435	2.93±0.03
0.200	1.31±0.03	0.350	2.34±0.03	0.450	3.01±0.03

It has been noted[20,4] that the normal-mode frequencies of nickel bear a roughly constant ratio to those of copper. A direct comparison of the results of Tables I and II with those of Ref. 20 gives an average value ≈ 1.24 for the ratio $\nu_{\mathrm{Ni}}/\nu_{\mathrm{Cu}}$. However, appreciable deviations (up to about 20% for the low-ζ part of the $[0\zeta\zeta]T_1$ branch) from this average value do occur. Using the Lindemann melting criterion one finds that

$$[(T_m/Ma^2)_{\mathrm{Ni}}/(T_m/Ma^2)_{\mathrm{Cu}}]^{1/2}=1.205,$$

which agrees quite well with the above value. (T_m is the melting temperature, M the atomic mass, and a the lattice constant.)

The results of Table I are plotted in Fig. 3 to give the dispersion relation for copper in the major symmetry directions. The diagram is labeled with the group-theoretical notation of Koster,[21] and the coordinates of $\mathbf{q}$ for the major symmetry points are shown at the bottom. The solid curved lines are the result of a fourth-neighbor general force constant analysis of the data of Table I which is discussed more thoroughly in the next section. These curves give an excellent fit to the data intersecting all but six of the experimental values inside the given errors—this in itself is evidence that the quoted errors are overestimates in the sense of standard deviations. The dashed lines for the II and Λ

[17] A. P. Miller, B. N. Brockhouse, and J. M. Rowe, Phys. Canada **22**, 24 (1966).
[18] B. N. Brockhouse, T. Arase, G. Caglioti, K. R. Rao, and A. D. B. Woods, Phys. Rev. **128**, 1099 (1962).
[19] A. D. B. Woods, B. N. Brockhouse, R. H. March, A. T. Stewart, and R. Bowers, Phys. Rev. **128**, 1112 (1962).
[20] R. J. Birgeneau, J. Cordes, G. Dolling, and A. D. B. Woods, Phys. Rev. **136**, A1359 (1964).
[21] G. F. Koster, in *Solid State Physics*, edited by F. Seitz and D. Turnbull (Academic Press Inc., New York, 1957), Vol. 5, p. 173.

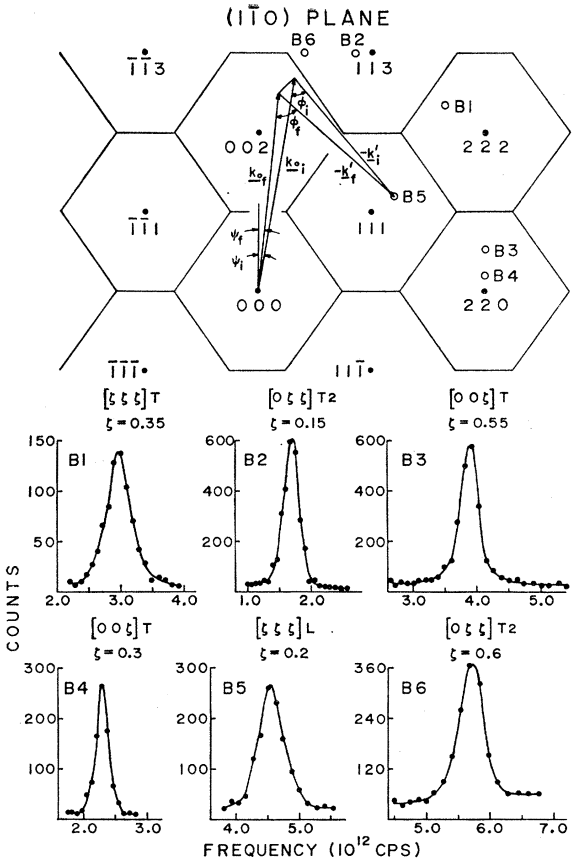

FIG. 2. The (1$\bar{1}$0) plane of the reciprocal lattice and several typical neutron groups for copper obtained in "constant-Q" experiments such as the one shown for group B5. The groups are labeled with the branch designation and the value of the reduced wave vector ζ.

branches are constructed from the known symmetry about W. The straight lines drawn from the points Γ represent the velocities of sound for the various branches calculated from the elastic constants of Overton and Gaffney[22] (see Table III). The points nearest Γ on all except the $[0\zeta\zeta]T_1$ branch agree very well with the velocity of sound values. The points on the T_1 branch are significantly high.

In Fig. 4 the low-wave-vector region of the $[0\zeta\zeta]T_1$ branch is shown together with a typical neutron group measured with the McMaster spectrometer. (After the original study, five groups on the low-ζ part of this branch were remeasured with the vertical collimation increased by about a factor of 3. It was found that for $\zeta \lesssim 0.3$ the original frequencies were lowered by about 0.015×10^{12} cps; the values of Table II have been corrected accordingly, but the points plotted in Fig. 4 represent the original uncorrected values. The groups taken with the higher vertical resolution were also about 20% narrower. The higher energy resolution and the increased vertical collimation used in the experiments at McMaster University easily account for the frequencies in Table II being slightly lower than the corresponding frequencies in Table I.)

The T_1 branch is of particular interest for several reasons: (i) It is very nearly a straight line up to at least $\zeta=0.5$. (There is evidence for this in Fig. 1 where it is seen that the neutron groups for $\zeta=0.2$ and 0.5 have almost equal widths which implies that the slope of the dispersion curve is almost identical for the two values of ζ.) (ii) The slope of this almost straight line is about 5% greater than the velocity of sound for this branch which is determined by the shear elastic constant $C'=(c_{11}-c_{12})/2$. (This does not necessarily imply that either the elastic constants[22] or the neutron-scattering results are incorrect since the elastic constant measurements correspond to very much smaller velues of ζ than any of the neutron results.) (iii) The ratios of the nickel to the copper frequencies are highest for the low-ζ part of this branch. (iv) The low-ζ part of this branch in palladium[17] has been found to have an anomalous S shape. (v) A Kohn anomaly[18] might possibly appear in this branch at $\zeta\approx0.45$, corresponding to transitions across the "belly" of the Fermi surface.[23]

The low-ζ part of the T_1 branch thus appears to be

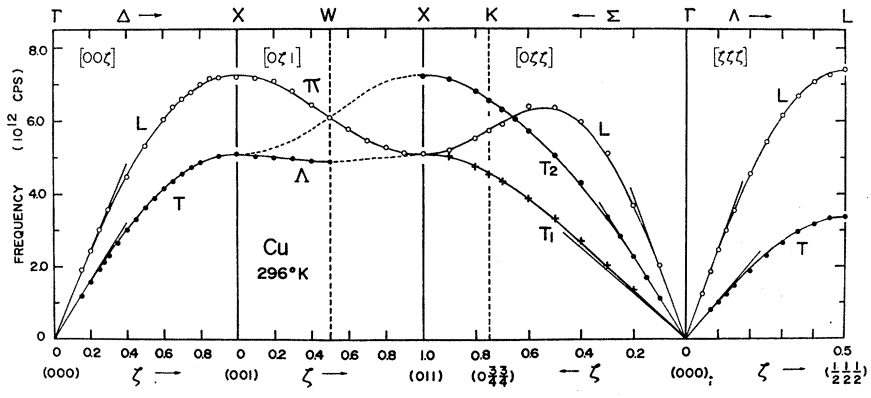

FIG. 3. The dispersion curves for copper in the four major symmetry directions at 296°K. The diagram is labeled with the group-theoretical notation of Koster (Ref. 21) and the straight lines through the points Γ give the initial slopes of the dispersion curves as calculated from the elastic constants (Table III). The solid and dashed curves are the result of an analysis in terms of general forces to 4th-nearest neighbors (model M1 of Table IV).

[22] W. C. Overton, Jr., and J. Gaffney, Phys. Rev. 98, 969 (1955).
[23] B. Segall, Phys. Rev. 125, 109 (1962).

TABLE III. Some physical constants of copper at 296°K.

Mass = 63.54 amu
Lattice constant = 3.6147 Å (face-centered cubic)
Elastic constants in units of 10^{11} dyn/cm^2:
$c_{11}=16.85\pm0.2\%$, $c_{12}=12.15\pm0.44\%$, $c_{44}=7.55\pm0.25\%$

somewhat of a "misfit" among the results for copper and also for palladium.[17] The straightness of the dashed line in Fig. 4 (which does not represent any fitting procedure) indicates that there is no significant S effect in copper. There is no evidence for the existence of a Kohn anomaly.

A search has also been made for a Kohn anomaly in the $[0\zeta\zeta]L$ branch; one might conceivably appear near $\zeta=0.22$ corresponding to transitions across the "neck" of the Fermi surface.[23] The slope, $(\nu_j-\nu_i)/(\zeta_j-\zeta_i)$, of the low-$\zeta$ part of this branch is shown in Fig. 5. Points are shown for $j=i+1$ and $j=i+2$, and are plotted at the positions $\zeta_{ji}=(\zeta_j+\zeta_i)/2$. A different notation is used for different sets of measurements—i.e., Chalk River "constant-**Q**", McMaster "constant-E" etc. Since it was necessary to relax the energy resolution in order to measure this branch under good focusing conditions [beyond the point (022) in Fig. 1], and since the focusing is never complete for longitudinal branches, the widths of the neutron groups for the lowest values of ζ are not negligible compared with the phonon frequencies. Nontrivial corrections are then required in order to obtain the correct phonon frequencies, so we have omitted the results of this study from Tables I and II. However, the measurements are adequate for detecting any abrupt changes in slope—i.e., Kohn anomalies. Within the sensitivity no anomaly was observed.

In Table III some relevant physical constants for copper are listed.

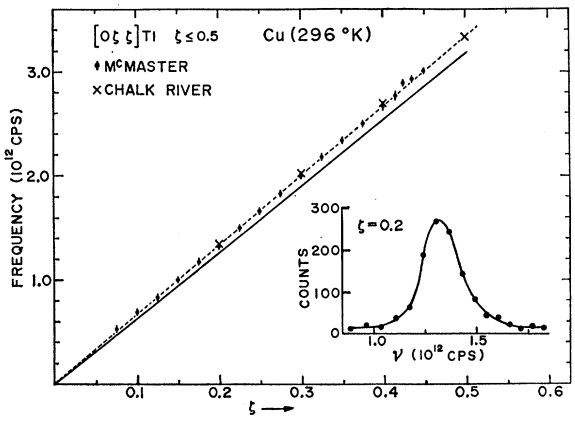

FIG. 4. The low-wave-vector part of the $[0\zeta\zeta]T_1$ branch and a typical neutron group measured with the McMaster spectrometer. The solid straight line is the velocity of sound calculated from the elastic constants (Table III). The results for $\zeta\leq0.3$ have not been corrected for the effects of vertical resolution and are probably too high by about 0.015×10^{12} cps.

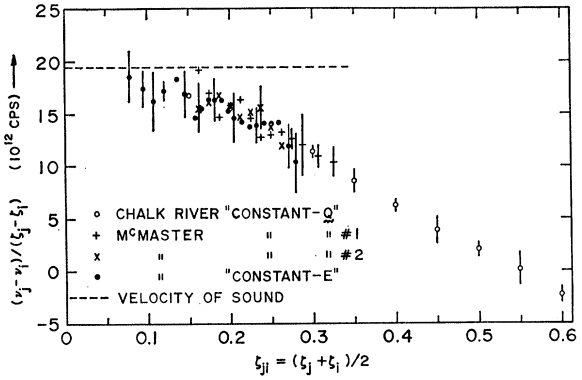

FIG. 5. The slopes for the low-wave-vector part of the $[0\zeta\zeta]L$ branch. The points labeled (McMaster "constant-**Q**" #1) refer to measurements beyond the point (022) in Fig. 1, and those labeled (McMaster "constant-**Q**" #2) refer to measurements before this reciprocal lattice point. The initial slope as given by the elastic constants is shown as a dashed line.

III. ANALYSIS OF RESULTS AND DISCUSSION

A. Force-Constant Models

An extensive analysis has been carried out in an attempt to determine the best possible force-constant model(s) from the measured frequencies and to assign physically realistic errors to the atomic force constants. A detailed discussion of this analysis is given in Appendix A; the main results are outlined in this section.

Several force-constant models (M1–M5) determined from the results are given in Table IV together with the sixth-neighbor general force-constant model (M6) of Sinha.[4] Various other models have been proposed for copper,[9,24–26] but the present work and that of Sinha both show that these models are inadequate. We will not consider them further. The atomic force constants $-\Phi_{\alpha\beta}(\mathbf{R}_L)$ of Eq. (4) are here written in the notation indicated by the matrix of Table IV where n refers to nth-nearest neighbors. Errors are assigned to each force constant for models M2–M4; these errors are determined by the errors assigned to the measured frequencies and elastic constants and the weights assigned to any constraints imposed during the least-squares fitting procedure. The mathematical procedure for calculating the errors in the force constants is outlined in Appendix B. As outlined in Appendix A, these errors are only physically significant if an adequate fit to the data is obtained. We have previously suggested that the quoted errors in the measured frequencies are probably two standard deviations; in this case so are the quoted force-constant errors.

An adequate fit to the measurements is not obtained

[24] G. W. Lehman, T. Wolfram, and R. E. DeWames, Phys. Rev. **128**, 1593 (1962).
[25] R. E. DeWames, T. Wolfram, and G. W. Lehman, Phys. Rev. **131**, 528 (1963).
[26] H. C. White, Phys. Rev. **112**, 1092 (1958).

TABLE IV. Atomic force constants for copper at 296°K in units of 10^4 dyn/cm.

AFC	M1	M2	M3	M4	M5	M6
$1XX$	1.3109	1.3141±0.0110	1.3102±0.0120	1.3160±0.0192	1.3224	1.3478
$1ZZ$	−0.1315	−0.1229±0.0150	−0.1417±0.0186	−0.1489±0.0330	−0.1570	−0.1215
$1XY$	1.5037	1.4983±0.0203	1.4820±0.0240	1.4880±0.0337	1.4794	1.4982
$2XX$	0.0215	0.0062±0.0224	0.0361±0.0246	0.0453±0.0295	0.0278	0.0018
$2YY$	−0.0251	−0.0106±0.0140	−0.0238±0.0147	−0.0345±0.0170	−0.0170	−0.0048
$3XX$	0.0529	0.0444±0.0072	0.0642±0.0103	0.0573±0.0228	0.0758	0.0507
$3YY$	0.0279	0.0317±0.0059	0.0315±0.0068	0.0321±0.0117	0.0229	0.0239
$3YZ$	0.0014	−0.0175±0.0077	0.0190±0.0133	0.0252±0.0154	0.0176	0.0159
$3XZ$	0.0400	0.0358±0.0045	0.0385±0.0052	0.0342±0.0077	0.0353	0.0378
$4XX$	−0.0024	−0.0064±0.0064	0.0104±0.0080	0.0099±0.0089	0.0118	0.0267
$4ZZ$	−0.0310	−0.0462±0.0110	−0.0284±0.0132	−0.0190±0.0154	−0.0296	−0.0032
$4XY$	−0.0043	0.0066±0.0093	0.0396±0.0206	0.0424±0.0301	0.0414	−0.0036
$5XX$			−0.0137±0.0058	−0.0121±0.0195	−0.0212	−0.0110
$5YY$			0.0009±0.0074	0.0015±0.0086	−0.0006	−0.0203
$5ZZ$			−0.0016±0.0079	0.0032±0.0114	0.0019	0.0037
$5XY$			−0.0055±0.0032	−0.0051±0.0097	−0.0077	0.0018
$6XX$			−0.0138±0.0063	−0.0111±0.0079	−0.0095	−0.0157
$6YZ$			−0.0232±0.0087	−0.0337±0.0134	−0.0265	−0.0058
$7XX$				0.0031±0.0102	0.0018	
$7YY$				0.0039±0.0111	0.0000	
$7ZZ$				−0.0089±0.0048	−0.0010	
$7YZ$				0.0009±0.0012	0.0007	
$7XZ$				0.0013±0.0018	0.0010	
$7XY$				0.0026±0.0036	0.0021	
$8XX$				−0.0201±0.0123	−0.0048	
$8YY$				0.0054±0.0088	0.0018	

Constraints

M1 and M2 General forces
M3 $8(5XY)=3(5XX)-3(5YY)$
M4 $8(5ZZ)=9(5YY)-5XX$; $3(7YZ)=7XY$
$8(5XY)=3(5XX)-3(5YY)$; $2(7XZ)=7XY$
M5 Axially symmetric forces
M6 General forces—S. K. Sinha (Ref. 4)

Force-constant matrix

$$\begin{pmatrix} nXX & nXY & nXZ \\ nXY & nYY & nYZ \\ nXZ & nYZ & nZZ \end{pmatrix}$$

Reference atoms
$(a/2)(hk\ell)$, $h\geq k\geq \ell\geq 0$

until at least sixth-nearest neighbors are included, hence the errors given in M2 are too small. M1 and M2 are fourth-neighbor general force-constant models which represent fits to the data of Table I and all the data, respectively. M1 was used to calculate the solid and dashed curves of Fig. 3. The force constants for these two models do not agree within the errors given in M2; this is expected since different data were used for the two models, since the errors in M2 are too small, and especially since a different weighting procedure was followed in obtaining the two models (see Appendix A).

There is not sufficient orthogonal information in measurements made only along the symmetry directions to do a completely general force-constant analysis beyond fourth neighbors. When fifth neighbors are included it is necessary to impose one constraint in order to separate $5XY$ from $1XY$ and $4XY$ (otherwise we have only two independent equations in these three unknowns). For M3 we have imposed the axially-symmetric[24] constraint $8(5XY)=3(5XX)-3(5YY)$. The particular constraint imposed affects the values of $1XY$, $4XY$, $5XY$, and especially their errors, so we cannot say with certainty that the errors assigned to these three force constants are physically realistic. Fortunately, the particular constraint imposed does not affect the values of the other 15 force constants in M3 or their errors, and, since M3 represents an adequate fit to the data, these errors are probably physically realistic. The first-neighbor force constants, which are quantitatively determined, are dominant; they indicate strong forces between first-nearest neighbors which probably arise from the interaction of the d shells on adjacent copper ions. The force constants for more distant interactions, none of which are much larger than 4% of $1XY$, are at best a few times as large as their errors. There is a weak long-range force system in copper about which we can say little except that it exists and extends to at least sixth-nearest neighbors. This is the expected effect of the conduction electrons in copper.

Sinha[4] measured a great many off-symmetry frequencies and fitted his results by a model involving general forces extending to sixth neighbors—model M6 of Table IV. Comparing M3 and M6, we see that there is in general good agreement. Sinha has not assigned errors to his force constants and in fact does not attach any physical significance to these force constants, but rather gives them as an interpolation formula. We feel that his force constants do have physical significance and should have errors somewhat larger than those of M3 because of the larger values of $\Delta\nu$ assigned to his measured frequencies. The force constants of M3 and M6 would then agree within the combined errors. We have previously mentioned the importance of the agreement between our measured frequencies and Sinha's

TABLE V. Interplanar force constants Φ_n for copper at 296°K in units of 10^4 dyn/cm.[a]

Branch	Φ_0	Φ_1	Φ_2	Φ_3	Φ_4	Φ_5	Φ_6	Φ_7	Φ_8
[00ζ]L	···	10.94±0.17 10.99(10.91)	0.49±0.16 0.56(0.60)	−0.07±0.15 −0.11(−0.05)	0.14±0.15 ··· (−0.04)	−0.02±0.15	0.01±0.15	−0.09±0.15	0.06±0.14
[00ζ]T	···	5.41±0.08 5.38(5.40)	0.02±0.07 0.02(0.02)	−0.03±0.06 −0.00(−0.02)	0.00±0.06 ··· (0.01)	−0.02±0.06	0.02±0.07	−0.01±0.07	−0.00±0.06
[0ζζ]L	···	4.60±0.12 4.75(4.75)	5.80±0.18 5.74(5.79)	0.72±0.17 0.63(0.58)	−0.09±0.15 −0.10(−0.16)	0.10±0.17 ··· (0.05)	−0.02±0.17	−0.10±0.16	0.07±0.17
[0ζζ]T_1	···	5.36±0.09 5.36(5.35)	−0.40±0.07 −0.39(−0.39)	0.05±0.06 0.01(0.02)	−0.06±0.06 −0.02(−0.04)	0.00±0.06 ··· (0.01)	0.05±0.07	−0.03±0.07	0.01±0.06
[0ζζ]T_2	···	10.61±0.21 10.62(10.64)	−0.09±0.18 −0.05(−0.08)	0.32±0.14 0.26(0.29)	−0.06±0.13 −0.12(−0.06)	−0.08±0.14 ··· (−0.07)	0.02±0.15	−0.03±0.15	0.05±0.15
[ζζζ]L	···	11.26±0.20 11.22(11.21)	0.50±0.18 0.68(0.69)	−0.02±0.17 −0.12(−0.13)	−0.01±0.17	0.04±0.17	−0.03±0.17	0.02±0.17	−0.07±0.18
[ζζζ]T	···	2.36±0.06 2.35(2.35)	−0.09±0.05 −0.07(−0.06)	0.00±0.05 0.02(0.02)	0.01±0.05	0.02±0.05	−0.00±0.05	−0.00±0.05	0.01±0.05
[0ζ1]Π	21.52±0.72 21.77(21.73)	−5.57±0.26 −5.50(−5.59)	−0.37±0.23 −0.48(−0.40)	0.11±0.22 −0.01(0.11)	0.12±0.22 ··· (0.01)	0.09±0.23	0.05±0.22	−0.02±0.21	−0.01±0.23
[0ζ1]Δ	10.74±0.34 10.75(10.76)	···	−0.36±0.19 −0.47(−0.44)	···	0.01±0.18 ··· (−0.04)	···	−0.06±0.18	···	−0.06±0.19

[a] The numbers in the second line for each branch are the appropriate sums of atomic force constants for models M3 and M4 (in brackets).

symmetry-direction frequencies in view of the different experimental methods used. (Sinha used a time-of-flight spectrometer.) The agreement between M3 and M6 is also very important because Sinha's model was determined primarily from off-symmetry measurements, and M3 was determined completely from measurements in symmetry directions.

M4 represents the best possible mathematical fit to the measurements using forces extending to 8th neighbors. However, it is little better than M3 for copper, and may have less physical significance since all but 10 of the 26 force constants are directly affected by the four constraints imposed (which are listed at the bottom of Table IV). M5 is an eighth-neighbor axially symmetric model which gives a poorer fit than does M3. For this and other reasons (see Appendix A) we feel that the forces in copper are probably not exactly axially symmetric. (They are not central since the Cauchy relation is not satisfied.)

The interplanar force constants Φ_n for each of the nine symmetry branches presented here are given in Table V together with the appropriate sums of atomic force constants[27] for models M3 and M4. The agreement between the Φ_n and these sums is usually inside the errors of the Φ_n indicating that models M3 and M4 give an adequate fit to each branch as well as to the entire symmetry-direction dispersion relation. When errors are calculated for the force constant sums, the agreement is always inside the combined errors. The errors in Table V have the same meaning as those in Table IV but are larger because of the smaller overdeterminacy in the interplanar fits.

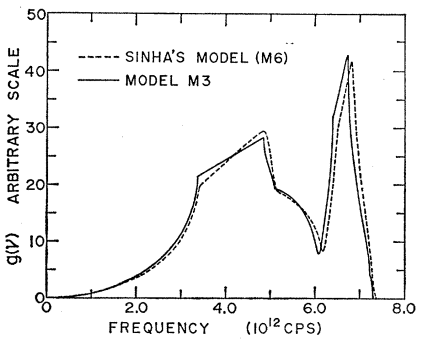

FIG. 6. The frequency distribution for copper from model M3 (solid curve) and from Sinha's model M6 (dashed curve). The two distributions are normalized to the same area.

B. Frequency Distributions

Frequency distributions have been calculated for each of the models M1–M4. The distribution for M1 was calculated by the method of Gilat and Dolling[13] using the program at Chalk River. The calculation gave an effective number of frequencies equal to 35 831 808 in the first Brillouin zone; the procedure was identical with that used for nickel[20] and is described in detail in Appendix A of that paper. The distributions for models M2, M3, and M4 were kindly calculated for us by Dr. L. J. Raubenheimer at Oak Ridge National Laboratory using the program described in Ref. 14. These three distributions are each normalized to 10^{10} effective frequencies. The four distributions are quite similar. The exact positions of the critical points, their relative magnitudes, and the curvatures of the sections between the various critical points are, however, slightly model-dependent.

The frequency distribution for M3 and for Sinha's model[4] M6 are shown in Fig. 6 as smooth curves drawn through the histograms[28] calculated with a "bin-width" of 0.01×10^{12} cps for M3 and 0.035×10^{12} cps for M6.

[27] See Ref. 18 for an interplanar decomposition in terms of atomic force constants to 5th-nearest neighbors; a table to 8th-nearest neighbors is available on request.

[28] Tables of numerical values for the frequency distributions calculated from models M1–M4 are available on request.

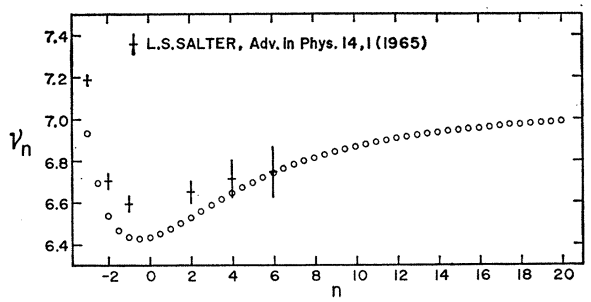

FIG. 7. Comparison of the Debye frequencies ν_n determined from model M3 and from experimental thermodynamic results by Salter. Salter's results are for 0°K whereas the M3 results are for 296°K (see text).

The distributions are normalized to the same area, and the agreement is quite good as expected from the agreement of the force constants in Table IV. The critical points displayed may be correlated with the stationary values and crossover points of the dispersion relation (Fig. 3). Other estimates of $g(\nu)$ for copper are given in Refs. 9 and 29–32; however, these are based on unrealistic models.

The moments of the frequency distributions have been calculated for $-3\leqslant n\leqslant 34$, but, since they vary in magnitude over a range $\approx 10^{30}$, it is more convenient to present the Debye frequencies ν_n given by Eqs. (8). A plot of the ν_n for the M3 distribution for $-3\leqslant n\leqslant 20$ is shown in Fig. 7 together with the results of Salter[33] obtained from experimental thermodynamic data. Salter's results are for the equilibrium volume at 0°K in the quasiharmonic approximation and are therefore higher than our results calculated from a room-temperature $g(\nu)$. The two sets of results do however have the same general shape throughout the range of overlap and can be brought into quite good agreement by approximate corrections for anharmonic effects. For example, using the values 1.96 and 1.63 for the thermodynamic Grüneisen parameter for copper,[34] and the value 14.09×10^{-6}/deg for the linear expansion coefficient,[35] one estimates that Salter's results should be decreased by 2.0–2.5%. This estimate is probably not very accurate; a much better correction to ν_{-3} is obtained by calculating the value of $\Theta_D(0°\mathrm{K})$, the Debye temperature at 0°K, which corresponds to the room-temperature elastic constants and lattice constant of Table III. Using the method of de Launay,[36] one finds that this value is 332.7°K, which corresponds to $\nu_{-3}=6.932\times10^{12}$ cps [see Eq. (8c)]. The 0°K elastic constants[22] and lattice constant give the value[36] $\Theta_D(0°\mathrm{K})=345.3°\mathrm{K}$ ($\nu_{-3}=7.194\times10^{12}$ cps), which agrees very well with the value $\omega_{-3}=4.518\pm0.014\times10^{13}$ rad/sec ($\nu_{-3}=7.191\pm0.022\times10^{12}$ cps) given by Salter.[33] It appears that Salter's value for ν_{-3} should be decreased by about 3.6%. If this correction is applied, there is excellent agreement with the values [ν_{-3} in the range $(6.921\text{–}6.932)\times10^{12}$ cps] for models M2–M4. The value for M1 is about 2% higher because M1 gives elastic constant values which are significantly higher than the experimental room-temperature values.[22]

The ν_n for $n>-3$ are not so easily corrected, but, from the agreement obtainable at $n=-3$, and the agreement in shape of the curves of Fig. 7, we feel that the over-all agreement is adequate. The ν_n for models M1–M4 are very similar, exhibiting only the above-mentioned differences arising from the different elastic constants corresponding to the different models, and small differences at larger n (0.5% at $n=20$) arising from the different "cutoff" frequencies of the different models. The ν_n for copper are quite different from those for nickel,[20] which are relatively much higher for negative n and which increase very slowly for $n\gtrsim5$.

Note added in manuscript: A complete description, including a FORTRAN 63 source language listing, of the Oak Ridge frequency distribution program is now available as an Oak Ridge National Laboratory report (ORNL-TM-1425 by L. J. Raubenheimer and G. Gilat). Recently this program has been rewritten in FORTRAN IV for use on the IBM 7040 computer at McMaster University. Modifications, which significantly improve the accuracy of the distributions at low frequencies (by as much as a factor of 3 for the first bin of the histogram) and which completely eliminate the negative frequencies given by the original program, have also been made at McMaster. The frequency distributions now obtained are essentially Debye distributions [$g(\nu)=a\nu^2$] at low frequencies. The accuracy of the $g(\nu)$ calculation for higher frequencies may be checked by comparing the value of the second moment obtained from the $g(\nu)$ histogram via Eq. (7) with the value obtained directly from the atomic force constants. For a face-centered cubic substance, the second moment may be expressed in terms of the atomic force constants as

$$M_2=(2\pi^2M)^{-1}\{2[2(1XX)+1ZZ]+2XX+2(2YY)+4[3XX+2(3YY)]+2[2(4XX)+4ZZ]+4[5XX+5YY+5ZZ]+4(6XX)+8[7XX+7YY+7ZZ]+8XX+2(8YY)+\cdots\},$$

where M is the atomic mass, and the notation is the same as in Table IV. For both the original and the improved $g(\nu)$ programs, the two values of M_2 agree to within 0.006%.

[29] P. A. Flinn, G. M. McManus, and J. A. Rayne, Phys. Rev. **123**, 809 (1961).
[30] K. C. Sharma and S. K. Joshi, Phys. Rev. **132**, 559 (1963).
[31] P. L. Srivastava and B. Dayal, Phys. Rev. **140**, A1014 (1965).
[32] Y. P. Varshni and R. C. Shukla, J. Chem. Phys. **43**, 3966 (1965).
[33] L. S. Salter, Advan. Phys. **14**, 1 (1965).
[34] C. Kittel, *Introduction to Solid State Physics* (John Wiley & Sons, Inc., New York, 1956), 2nd ed., p. 155.
[35] *Handbook of Chemistry and Physics*, edited by C. D. Hodgman *et al.* (The Chemical Rubber Publishing Company, Cleveland, Ohio, 1960), 42nd ed., p. 2241.
[36] Jules de Launay, in *Solid State Physics*, edited by F. Seitz and D. Turnbull (Academic Press Inc., New York, 1956), Vol. 2, p. 219.

C. Thermal Properties

The Debye temperature $\Theta_D(T)$ for $0°K \leqslant T \leqslant 300°K$, calculated using Eqs. (10) and (12) and the M3 frequency distribution, is shown in Fig. 8 together with the experimental results of various workers.[37–40] Where the values of $\Theta_D(T)$ were not given, we have calculated them using the value (0.688 mJ/mole deg^2) of Corak *et al.*[41] for γ, the electronic specific-heat coefficient, to subtract off the electronic specific heat. Our calculated $\Theta_D(T)$ (solid line) is almost always lower than the experimental values; this is expected since we have used a room temperature $g(\nu)$ to calculate $C_v(T)$ and $\Theta_D(T)$ for all T without making any corrections for anharmonic effects. Equation (11) for $C_v(T)$ is obtained under the assumptions $d\nu/dT=0$ and $dg(\nu)/dT=0$, and the experimental points of Fig. 8 are obtained from the specific heats by assuming that the value of γ determined at very low temperatures is valid for all temperatures. In view of the fact that none of these assumptions are justified, the agreement shown in Fig. 8 is as good as can be expected. The correct shape of the calculated curve is more significant than the fact that it is too low. As mentioned in the last section, we are low by just the amount we expect at 0°K since the room temperature elastic constants and lattice constant give $\Theta_D(0°K)=332.7°K$, and models M2–M4 give values of $\Theta_D(0°K)$ in the range 332.2–332.7°K. (M1 gives a value 338.6°K because the M1 elastic constants are too high.) Martin[40] gives $\Theta_D(0°K)=345.6°K$, and quotes the value 345.2°K as the best value obtained from 0°K elastic constants. Above about 15°K, models M1–M4 give results which differ from each other by less than 1°K ($\approx 0.3\%$). Due to the errors in the primary data, and the possible errors introduced in calculating the force constants, $g(\nu)$, $C_v(T)$, $\Theta_D(T)$, etc., it is difficult to make useful estimates of anharmonic corrections from the results given in Fig. 8.

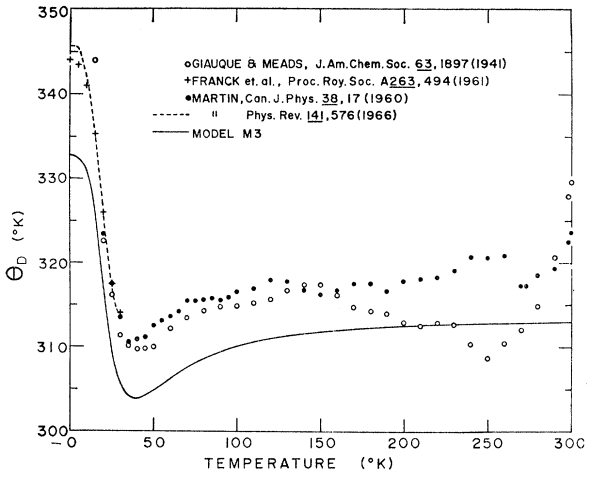

FIG. 8. Comparison of calculated (M3) and experimental values of the Debye temperature (see text).

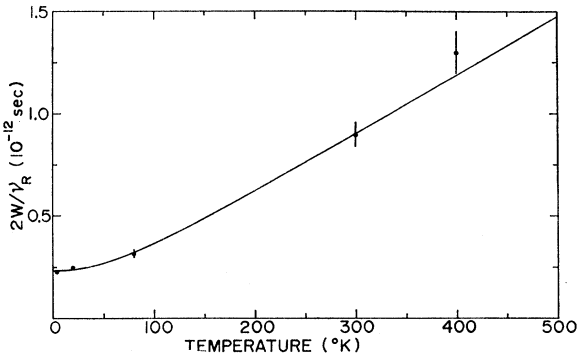

FIG. 9. Comparison of calculated (M1) and experimental (Ref. 29) values of the Debye-Waller coefficient divided by the recoil frequency ν_R of a free copper atom.

The Debye-Waller coefficient $2W(T)$ has also been computed. The calculated curve for $2W(T)/\nu_R$ [see Eq. (11)] is shown in Fig. 9 together with the experimental results (from x-ray intensity measurements) of Flinn *et al.*[29] taken from Ref. 25. The results for models M1–M4 never differ by more than 0.8% over the range shown.

IV. CONCLUSIONS

It has been demonstrated that the 1st-neighbor interactions in copper are dominant, and that there exists a weak longer range force system extending to at least 6th-nearest neighbors. Physically realistic errors have been assigned to most but not all of the force constants. Our force constants agree substantially with those of Sinha, but disagree with earlier estimates. The analysis indicates that the forces in copper are not completely axially symmetric. The analysis has also indicated that the errors conventionally assigned to the frequencies obtained in neutron scattering experiments are too large by about a factor of 2, if the errors are to have the sense of standard deviations. When the Oak Ridge results[10] are available in final form, a statistical comparison with our results should give an answer to this important question. Unless the assigned errors differ from standard deviations by a constant factor, a least-squares method of analysis is of course not strictly justified.

No Kohn anomalies were observed in copper though they probably exist and might be seen at lower temperatures and/or under very high resolution.

Thermodynamic quantities calculated from the frequency distributions agree as well as can be expected with the experimental quantities; the small discrepan-

[37] W. F. Giauque and P. F. Meads, J. Am. Chem. Soc. **63**, 1897 (1941).
[38] J. P. Franck, F. D. Manchester, and D. L. Martin, Proc. Roy. Soc. (London) **A263**, 494 (1961).
[39] D. L. Martin, Can. J. Phys. **38**, 17 (1960).
[40] D. L. Martin, Phys. Rev. **141**, 576 (1966).
[41] W. S. Corak, M. P. Garfunkel, C. B. Satterthwaite, and A. Wexler, Phys. Rev. **98**, 1699 (1955).

cies (never more than 4%) appear to be accounted for by anharmonic effects.

ACKNOWLEDGMENTS

The authors wish to express their appreciation to the staff of Atomic Energy of Canada Limited at Chalk River, in particular to Dr. A. D. B. Woods, Dr. G. Dolling, Dr. R. A. Cowley, E. A. Glaser, A. Bell, and M. McManus, for their cooperation and assistance and for the use of equipment and computer programs. We also wish to thank Dr. L. J. Raubenheimer and Dr. R. M. Nicklow of Oak Ridge National Laboratory for sending us their preliminary results and for calculating several frequency distributions, and Dr. S. K. Sinha for sending us his results prior to publication.

APPENDIX A: DETAILED STUDY OF FORCE-CONSTANT MODELS

The atomic force constants (AFC's) were determined from the experimental frequencies by a least-squares analysis based on Eqs. (3) and (4). (In view of the somewhat arbitrary method of assigning errors to these frequencies, it is of course not certain that a least-squares method is fully justified.) Except for model M1 of Table IV, weights were assigned according to the least-squares prescription—i.e., the values of $M\omega_j^2$ were weighted relatively as $(\nu_j\Delta\nu_j)^{-2}$, and the values of (aC_i) were weighted accordingly (the C_i are the elastic constants, a is the lattice constant, and the ν_j and $\Delta\nu_j$ are the frequencies and errors of Tables I and II.) For model M1, the values of $M\omega_j^2$ were weighted relatively as $(\nu_j\Delta\nu_j)^{-1}$, and the values of aC_i were assigned rather low weights. This easily accounts for the differences between models M1 and M2. Although M1 was obtained from the data of Table I only, it actually gives a better fit to all the data of Tables I and II than does M2, but it fits the elastic constants much less well (see Table VI).

The force-constant errors given in Table IV for models M2–M4 are determined primarily by the errors assigned to the experimental frequencies and elastic constants. However, where constraints are imposed, the errors assigned to the force constants affected by these constraints are determined largely by the errors assigned to other force constants—e.g., the error assigned to the force constant $5XY$ of model M3 is determined largely by the errors assigned to the force constants $5XX$ and $5YY$ since $5XY$ is fixed by the constraint $8(5XY)=3(5XX)-3(5YY)$. The errors propagate in the standard way as long as fairly large weights are assigned to the constraints imposed. The constraints were also fitted by least squares since this allows one to test (by varying the weights assigned to the constraints and observing the changes in the fitting errors) if the data are consistent with the constraints. We have not found an adequate way to take account of truncation errors so, in calculating the errors in the force constants, we implicitly assume that we have a "perfect" model. The force-constant errors are therefore physically realistic only if an entirely adequate fit to the data was in fact obtained. Figure 10 shows a plot of Δ1, the weighted root-mean-square (rms) error in $M\omega_j^2+aC_i$, and Δ2, the unweighted rms error in ν_j, as functions of the number of neighbors (n) employed in the fits. These errors decrease very rapidly up to $n=3$, less rapidly to $n=6$, and then only very slowly to $n=8$, the limit of the analysis. Other errors (e.g., the fitting error and the average absolute error in ν_j) show the same type of behavior. We take this as an indication that forces to sixth-nearest neighbors are required, and are probably adequate, to fit the measurements. The errors given for model M2 are therefore too small. The errors increase from M2 to M3 to M4 because, as more parameters are added by including more distant neighbors, there is less "orthogonal" data to determine each parameter.

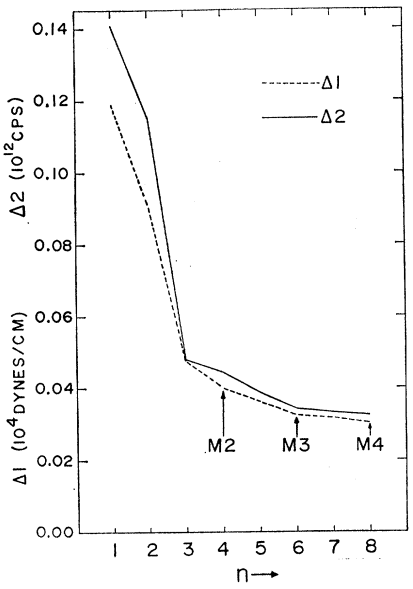

FIG. 10. The statistical quantities Δ1 and Δ2 [see Eqs. (A1) and (A2)] as a function of the number (n) of nearest neighbors included in the fit. The values for models M2, M3, and M4 of Table IV are indicated by arrows.

The errors assigned to the force constants will differ from standard deviations by the same factor that the errors in Tables I and II differ from standard deviations. Analysis suggests that the errors assigned are too large by about a factor of 2; this is arrived at as follows: Even with an exact theory, one would expect the frequencies calculated from the best force-constant model to be outside the assigned errors for $\frac{1}{3}$ of the experimental frequencies if these errors were standard deviations, and if there were a much larger number of data points than parameters. There are 124 data points in Tables I and II, and M4 gives frequencies that are outside the assigned errors for only 6 (i.e., for 5%) of

them, for M3 the number is 9 (7%), and even for M2 it is only 14 (11%). Even if we arbitrarily set $\Delta\nu=\frac{1}{2}\Delta\nu$ throughout, the numbers are only 31 (25%), 36 (29%), and 50 (40%) for M4, M3, and M2, respectively—a straightforward division by 2 does not appear to be too drastic a procedure. In addition, predicted and observed values of certain statistical quantities such as $\Delta 2$, the unweighted rms error in ν_j, can be compared. For predicted values one uses appropriate averages of the $\Delta\nu_j$ given in Tables I and II, and for observed values one replaces the $\Delta\nu_j$ by $(\nu_j{}^c-\nu_j)$, where the $\nu_j{}^c$ are the frequencies calculated from a particular model, and the ν_j are the measured frequencies. A comparison of the predicted and observed values of the quantities $\Delta 1-\Delta 4$

TABLE VI. The statistical quantities[a] $\Delta 1$–$\Delta 4$ calculated from the force-constant models M1–M5 and as predicted from the errors of Tables I and II.

	$\Delta 1$	$\Delta 2$	$\Delta 3$	$\Delta 4$
Predicted	···	0.0734	0.0673	0.0665
M1	0.0593	0.0358	0.0271	0.0408
M2	0.0400	0.0444	0.0316	0.0417
M3	0.0324	0.0342	0.0254	0.0338
M4	0.0302	0.0325	0.0234	0.0313
M5	0.0334	0.0354	0.0265	0.0353

[a] See Eqs. (A1)–(A4).

is given in Table VI. These quantities are defined as follows:

$$\Delta 1=\{[\sum_i w_i(y_i{}^c-y_i)^2]/W\}^{1/2}, \tag{A1}$$

$$\Delta 2=[N^{-1}\sum_i{}' (\nu_i{}^c-\nu_i)^2]^{1/2}, \tag{A2}$$

$$\Delta 3=N^{-1}\sum_i{}' |\nu_i{}^c-\nu_i|, \tag{A3}$$

and

$$\Delta 4=\{[\sum_i{}' w_i(y_i{}^c-y_i)^2]/W'\}^{1/2}, \tag{A4}$$

where $y_i=M\omega_i{}^2$ or aC_i, $y_i{}^c$ is the corresponding quantity calculated from a particular model, a primed summation is over the ($N=124$) values of $M\omega_i{}^2$, an unprimed summation is over these plus the three values of aC_i, $w_i=[\Delta(y_i)]^{-2}$, $W=\sum_i w_i$, and $W'=\sum_i{}' w_i$. One sees that the fits are better than expected by about a factor of 2. This strongly indicates that the errors assigned to the experimental frequencies are about two standard deviations. It is not a conclusive proof, however, because systematic errors could exist for several branches or parts of branches, and a good fit could still be obtained using the least-squares procedure. The fact that the measurements carried out at the Chalk River and McMaster reactors, using instruments of rather different characteristics, are in good agreement (for both palladium[17] and copper) suggests that systematic errors are in fact small. Independent data[4] exist for copper, but unfortunately they do not lend themselves to a meaningful statistical comparison such as is needed to fully justify decreasing the quoted errors. This is because Sinha's results[4] for the symmetry directions are unevenly spaced as to wave vector, branch, and direction, and his quoted errors are two to five times ours. However, the good agreement between his and our results where overlap occurs, and the good agreement between his force-constant model and frequency distribution and our models and distributions, argues that the errors assigned to experimental frequencies are being habitually overestimated. The Oak Ridge[10] data, when available in final form, will afford a better statistical comparison. The results available at present are in rather good agreement with ours except for certain limited regions of reciprocal space.

There is not sufficient orthogonal information in the four major symmetry directions of a face-centered cubic substance to allow one to carry out an analysis in terms of completely general forces if neighbors beyond fourth-nearest neighbors are included in the fit. It has become conventional to circumvent this problem by imposing axially symmetric (AS) or central-force constraints, and to then include sufficient neighbors to get an adequate mathematical fit. (The AS model is simply the central-force model without the requirement that all forces be derivable from the same potential.) Such models may be useful as interpolation formulas for calculating frequency distributions, etc., but the atomic force constants so obtained may not be physically realistic, since there is no reason to believe *a priori* that the forces in a particular substance are central or even AS. We have extended our analysis beyond fourth neighbors by a procedure which yields the maximum number of free parameters, hence giving the best mathematical fit, and which also allows one to assign physically realistic errors to the largest possible number of force constants. One constraint is required when 5th neighbors are included. (The symmetry directions give only two independent equations for the three force constants $1XY$, $4XY$, and $5XY$, so one of these must be fixed at some arbitrary value with arbitrary weight.) A reasonable procedure would be to fix one of these force constants by an AS constraint; this can be done in five ways—three ways for $5XY$ and one way for each of $1XY$ and $4XY$. Each of these AS constraints (as well as any other constraint that suffices to separate $5XY$ from $1XY$ and $4XY$) will yield identical fitting errors. There is of course no reason to believe that an AS constraint is more physically meaningful than any other type of constraint, or that any one of the five AS constraints is superior. An AS constraint does, however, force the AFC being fixed by that constraint to be of a reasonable magnitude; also, one intuitively expects $1XY$ to have stabilized before fifth neighbors are introduced, and certain of the AS constraints cause it to change only very slightly (see Table VII). (One might indeed have fixed $1XY$ at the value given by model M2 rather than

TABLE VII. The 6th-neighbor force-constant models for the five axially symmetric constraints that suffice to separate $5XY$ from $1XY$ and $4XY$.[a]

$1XY$	$4XY$	$5XY$	AS[b] constraint
1.4820±0.0240	0.0396±0.0206	−0.0055±0.0032	$8(5XY)=3(5XX)-3(5YY)$
1.4848±0.0237	0.0367±0.0183	−0.0040±0.0036	$3(5XY)=5XX-5ZZ$
1.5080±0.0905	0.0135±0.0856	0.0075±0.0443	$5XY=3(5YY)-3(5ZZ)$
1.4827±0.0280	0.0388±0.0152	−0.0051±0.0112	$4XY=4XX-4ZZ$
1.4519±0.0272	0.0696±0.0360	−0.0205±0.0174	$1XY=1XX-1ZZ$

[a] The other 15 force constants are identical to those given in model M3 of Table IV.
[b] Axially symmetric.

use an AS constraint.) The values of the three force constants $1XY$, $4XY$, and $5XY$, and especially of their errors, are dependent on the particular constraint imposed. Model M3 of Table IV gives the values for the AS constraint $8(5XY)=3(5XX)-3(5YY)$; in Table VII these values are listed again together with the values for the other four AS constraints. Because of the dependence on the particular constraint used (and the absence of a satisfactory criterion for choosing the "best" constraint), it is difficult to assign physically realistic errors to $1XY$, $4XY$, and $5XY$. The other 15 force constants and their errors in M3 are determined uniquely by the data, and, because this model gives an adequate fit to the data, the errors assigned are probably realistic. M3 is the most physically meaningful model obtained thus far for copper; it has seventeen mathematically free parameters, only one less than a completely general model, and hence gives a better fit to the data than a sixth-neighbor AS model with only 12 free parameters.

When seventh neighbors are included in the fit, three additional constraints must be imposed since the symmetry directions give only two independent equations in the three force constants $3YZ$, $6YZ$, and $7XZ$; three in the four force constants $3XZ$, $4XY$, $6YZ$, and $7YZ$; and seven in the eight force constants $1XX$, $1ZZ$, $3XX$, $3YY$, $5XX$, $5ZZ$, $7XX$, and $7YY$. (It is assumed that $5XY$ has previously been fixed by the constraint of M3.) We have chosen to remove the first two underdeterminacies by fixing $7XZ$ and $7YZ$, since $6YZ$ cannot be fixed by an AS constraint, and we want to retain general forces for the first through fourth nearest neighbors. Again we choose to use AS constraints, and $7XZ$ and $7YZ$ are fixed by the constraints $2(7XZ)=7XY$ and $3(7YZ)=7XY$. (Since the AS constraints are also fitted by least squares, and since $7XY$ and $7ZZ$, and their errors, are very well fixed by the symmetry direction data, it is most convenient to fix the other seventh-neighbor force constants in terms of these two whenever seventh-neighbor AS constraints are imposed.) In addition one of $5XX$, $5ZZ$, $7XX$, and $7YY$ must be fixed. Imposing the AS constraint $8(5ZZ)=9(5YY)-5XX$ leads to the best stabilization of the force constants, so we have chosen to use this constraint even though (by the propagation of errors among the force constants) the AS constraints that fix $7XX$ or $7YY$ in terms of $7XY$ and $7ZZ$ lead to smaller errors for several of the force constants.

For model M4, the three AS constraints given above and the one used previously for M3 have been imposed. Various other sets of four AS constraints could have been used (all yielding the same fitting errors), and again there is nothing special about AS constraints. Only ten of the force constants ($2XX$, $2YY$, $4XX$, $4ZZ$, $5YY$, $6XX$, $7ZZ$, $7XY$, $8XX$, and $8YY$) of M4, and their errors, are not affected by the particular constraints imposed, and only these ten can be said to be physically realistic with certainty. Although M4 gives a slightly better fit[42] to the data than does M3, M3 with 15 physically realistic force constants is probably more meaningful. Comparing M3 and M4 we see that only one of the force constants of M3 changes by as much as its given error when seventh and eighth neighbors are added, and this force constant ($6YZ$) is directly affected by two of the constraints imposed in M4, so the change is not significant.

M5 is an eighth-neighbor AS model. Force-constant errors are not given for M5 because the calculated errors are very strongly affected by the ten constraints imposed. M5 gives a slightly poorer fit to the data than does M3, so the higher Fourier components inherent in M5 are not needed to fit the copper data. If the force constants of M5 are compared with the force constants of M3 and M4 (and the errors of the latter are divided by a factor of 2 to get standard deviations as indicated earlier), then it appears that the forces in copper are probably not quite axially symmetric. If the various axially symmetric sums [e.g., $1XX-1ZZ-1XY$, $3XX-3YY-3(3YZ)$, etc.] are plotted against the number of neighbors included in the fit (n), there is generally a tendency to stabilize at values which are not zero, as they would be for AS forces, but which differ from zero by amounts little greater than the errors in the sums.

Since the calculated elastic constants are very sensitive to small changes in the long-range force constants, the values of the atomic force constants are quite insensitive to the weights assigned to the measured elastic constants. For models M2–M4, test runs were made with relative weights from 0–10 on the (aC_i) (with respect to the weights assigned to the $M\omega_j^2$), and for

[42] The importance of obtaining the best mathematical fit has recently been emphasized [G. Gilat and R. M. Nicklow, Phys. Rev. 143, 487 (1966)]; model M4 will give the best 8th-neighbor fit to the symmetry-direction data of any fcc substance.

values greater than 0.01 the AFC's never changed outside the errors given in Table IV. For values of 0.001 and less, a few AFC's for each model changed by slightly more than their assigned errors. The (aC_s) are fitted relatively better than the $M\omega_j^2$ (i.e., $\Delta 1$ of Table VI is less than $\Delta 4$) for relative weightings $\gtrsim 0.05$; however, it takes a value of approximately 0.5 to fit all three of the measured elastic constants within the assigned errors[22] (see Table III). The $M\omega_j^2$ tend to make the values of c_{11} and the shear constant C' too high. For the models M2–M4 given in Table IV, a relative weighting factor of 0.125 was used, and for these models C' is 4–5% higher than the experimentally determined value to which Overton and Gaffney[22] assign an error of 1.8%. This disagreement arises primarily from the disagreement between our measurements for the $[0\zeta\zeta]T_1$ branch and the velocity of sound determined by C'; however, it may not be significant since it is possible to get very good agreement with the measured elastic constants without seriously decreasing the quality of the fit to the experimental frequencies. There is no reason to suspect the elastic constant measurements of Overton and Gaffney,[22] since other measurements[43] are in good agreement with them.

In calculating the Φ_n of Table V, the appropriate elastic constant combination for each branch was assigned the same weight as the value of $M\omega^2$ for the lowest value of ζ on that branch (except for the II and Λ branches).

A data randomization method of analysis was also used for both the Φ_n and the AFC's—i.e., the experimental ν_j were changed to $\nu_j+\Delta\nu_j$, $\nu_j-\Delta\nu_j$, or ν_j in a completely random manner, and then the Φ_n and the AFC's were calculated. This was done for several different randomizations of the data, and it verified that, if the assigned values of $\Delta\nu_j$ are realistic, then the force constant errors of Tables IV and V are realistic. This is an alternative (but more cumbersome) procedure for assigning physically realistic errors to the force constants.

APPENDIX B: DETERMINATION OF FORCE-CONSTANT ERRORS

The procedure for assigning errors to the atomic and interplanar force constants is outlined in this section. The method is not new.[44]

From experiment one has $y_j=M\omega_j^2$ or aC_j, and, using the method of least squares, one sets

$$\frac{\partial}{\partial\Phi_{k'}}\{\sum_j w_j(y_j^c-y_j)^2\}=0, \tag{B1}$$

where

$$y_j^c=\sum_k \alpha_{kj}\Phi_k, \tag{B2}$$

k may be a multiple index [e.g., L, β of Eqs. (3) and (4)], the Φ_k are the force constants, the α_{kj} are coefficients involving trigonometric functions like $1-\cos\mathbf{q}\cdot\mathbf{R}_L$ [see Eq. (4)], and the w_j are the least-squares weights,

$$w_j=\sigma_j^{-2}=[\Delta(y_j)]^{-2}. \tag{B3}$$

Expanding Eq. (B1), and making use of Eq. (B2) and its derivative, one obtains the equation

$$\sum_j w_j y_j\alpha_{k'j}=\sum_k \Phi_k \sum_j w_j\alpha_{kj}\alpha_{k'j}. \tag{B4}$$

Setting

$$X_k=\sum_j w_j y_j\alpha_{kj}, \tag{B5}$$

and

$$A_{kk'}=\sum_j w_j\alpha_{kj}\alpha_{k'j}, \tag{B6}$$

and, making use of the fact that $A_{kk'}=A_{k'k}$, Eq. (B4) can be written in matrix form as

$$\mathbf{X}=\mathbf{A}\mathbf{\Phi} \quad \text{i.e.,} \quad \mathbf{\Phi}=\mathbf{A}^{-1}\mathbf{X}=\mathbf{B}\mathbf{X}. \tag{B7}$$

Therefore,

$$\Phi_k=\sum_n B_{kn}X_n=\sum_n B_{kn}\sum_j w_j y_j\alpha_{nj}, \tag{B8}$$

and, making use of Eq. (B3),

$$\left(\frac{\partial\Phi_k}{\partial y_j}\right)^2[\Delta(y_j)]^2=\sum_{n,n'} B_{kn}B_{kn'}w_j\alpha_{nj}\alpha_{n'j}. \tag{B9}$$

Finally, using Eq. (B6), one has

$$\sum_j\left(\frac{\partial\Phi_k}{\partial y_j}\right)^2[\Delta(y_j)]^2=\sum_{n,n'} B_{kn}B_{kn'}A_{nn'}$$
$$=B_{kk}=(A^{-1})_{kk}. \tag{B10}$$

The left-hand side of Eq. (B10) is, by definition, the error in Φ_k. Hence, the errors in the atomic and interplanar force constants are simply the appropriate diagonal elements of the inverse of the matrix whose elements are given by Eq. (B6). Any constraints imposed in obtaining the models presented in this article were treated as additional input data (y_j) and were assigned a weight (w_j).

[43] J. A. Rayne, Phys. Rev. **112**, 1125 (1958); Y. Hiki and A. V. Granato, *ibid.* **144**, 411 (1966).

[44] See, e.g., H. D. Young, *Statistical Treatment of Experimental Data* (McGraw-Hill Book Company, Inc., New York, 1962), Chap. IV.